The Synchronic Frame of Photospheric Magnetic field: The Improved Synoptic Frame

X. P. Zhao, J. T. Hoeksema and P. H. Scherrer
W. W. Hansen Experimental Physics Laboratory, Stanford University

Short title: SYNCHRONIC FRAMES

Abstract.

It is shown that because of the effect of the differential rotation, the magnetic elements in a Carrington synoptic chart can not be used to fill up the entire solar surface at any time within the period of one solar rotation. By correcting the effect of the differention rotation included in synoptic charts, the improved synoptic chart, the "synchronic map", becomes a proxy of truely whole solar surface distribution of the photospheric magnetic field in the heliographic coordinate system. The improved synoptic frame, the "synchronic frame" obtained based on the synchronic map, has been shown to be a better proxy for the instantaneous whole surface distribution of the photospheric field at the time of interest. The coronal holes and the base of the heliospheric current sheet reconstructed using the synchronic frame appear to be better than that using the synoptic frame.

1. Introduction

The Carrington synoptic chart of the photospheric magnetic field (Bumba and Howard, 1965) is made from consecutive magnetograms observed over one Carrington rotation period. Each magnetogram is remapped and sliced a strip centered at the central meridian passing (CMP) time, and all obtained strips are ranged from right to left in the order of CMP time, and from left to right in the order of the Carrington longitude (Carrington, 1863) (see the top panel and the bottom and top abscissa of the middle panel in Figure 1). If the width of the strips equals to the grid (pixel) size of the magnetic synoptic chart, the magnetic synoptic chart is in fact a collection of the latitudinal distribution of magnetic elements along all centrial meridians observed at different CMP times over one Carrington rotation period. By implicitely neglecting the difference between the heliographic longitude and the Carrington longitudes (i.e., neglecting the effect of differential rotation) the magnetic synoptic chart has been assumed to be the entire solar surface distribution of the photospheric magnetic field, and used as an inner boundary condition of various data-based global coronal models for reconstructing global-scale, long-lived, coronal magnetic field and plasma structures, such as foot-points of open field lines or coronal holes (Levine, 1975) and the base of the heliospherical current sheet or the coronal helmat streamer belt (Hoeksema et al, 1983). The success of the reconstruction of global coronal structures implies that it is the underlying photospheric magnetic field that mainly responses for the overlying coronal structures (the same as the case of the locally modeling of local coronal structures). This success also shows that the magnetic synoptic chart at a Carrington rotation number may be grossly taken as a proxy of the entire surface field distribution for the specific Carrington rotation number.

Based on this practice and experience in coronal modeling, we have constructed the "synoptic frame", as a proxy of the instantaneous entire surface distribution of the photospheric magnetic field at the time of interest (the target time hereafter), to

track the change of transient large-scale coronal structures on the time scale much less than one solar rotation period (Zhao, Hoeksema and Scherrer, 1997). Here the target time is the observational time of interesting coronal structures. The synoptic frame consists of two components. One component is the target-time remapped magnetogram with central meridian angles of $\pm 50°$, which covers most part of the Earth-side solar surface; the other component is the east and west parts of the synoptic chart centered at the target time, which cover the farside and remaining Earth-side solar surface. We replace the term of "chart" with the term of "frame" to emphsize the major role played by the remapped magnetogram component in approximating the instantaneous entire surface field distribution and in tracking transient large-scale coronal structures. Figure 1 shows how the 1998:05:23_16:03:30 synoptic frame (see the bottom panel section) is constructed by replacing the central part of the synoptic chart centered at the target time of 1998:05:23_16:03:30 (see the middle panel with the abscissa expressed in Carrington longitudes for blue central meridian lines) with the 1998:05:23_16:03:30 remapped magnetogram (see the top panel with the abscissa expressed in heliographic longitudes for black meridian lines). The temporal variation of the 1996 August boot-shaped coronal hole boundary on the time scale of a day and the temporal variation of the 1994 April Soft X ray arcade on the time scale less than a day have been successfully reproduced using synoptic frames and various coronal magnetic field models (Zhao, Hoeksema and Scherrer, 1999; 2000).

It should be noted that all magnetic elements in the magnetogram component were observed at the target time, where the location of each meridian line was expressed as the heliographic longitude relative to the central meridian. In the synoptic chart component, however, the magnetic elements located at different meridian lines were observed at different CMP times and were expressed as Carrington longitude. As seen from the bottom panel of Figure 1, the abscissa of the synoptic frame is expressed in hybrid manner, i.e., using heliographic longitudes for the magnetogram component

and using Carrington longitudes for the synoptic-chart component. To make the abscissa of synoptic frames being expressed fully by heliographic longitudes and the field distribution becomes truely over the whole solar surface, this work tries to correct the effect of the differential rotation included in the synoptic chart so that the mapping inconsistence can be removed.

The differential rotation may introduce errors into the synoptic chart in two ways, as discussed in Ulrich and Boyden (2006) (UB06 hereafter). Firstly, the differential rotation cause magnetic elements to change their heliographic longitude as a function of observation time, and thus merges and averages over multiple strips observed at different times are smeared. Secondly, magnetic elements along a central meridian line at Carrington longitude (a CMP time) will be differentially shifted at the target time from their original meridian line. By introducing parameters of the "Carrington time" and the "Carrington-time equivelant longitude", Ulrich and Boyden (2006) carry out the correction of the differential-rotation effects.

In Section 2, we first describe how to using a slightly different method to make conversation between the Carrington longitude and the heliographic longitude, and to first obtain the improved synoptic chart, i.e., the synoptic chart without smearing effect and the "synchronic map", and then merge the remapped magnetogram with the synchronic map to obtain the improved synoptic frame, the "synchronic frame" in what follows. To see the effect of differential rotation on the distribution of the field strength and polarity structures, we compare the synchronic frame with the synoptic frame in Section 3. In Section 4 we show the effect of differential rotation on modeled coronal structures by comparing the coronal structures obtained using synchronic frames with that using synoptic frames, and by comparing the calculated results with observations. In the last section we summry the results and discuss the possibility of further improving the synchronic map and synchronic frame.

2. Construction of the synchronic chart and the synchronic frame

2.1. Denotation of the Carrington longitude and the heliographic longitude

The photospheric magnetic field on the solar surface is, in general, a function of the time t, the heliographic latitude λ, and the heliographic longitude ϕ, and can be expressed as $B(\lambda, \phi, t)$. Because of the differential rotation of photospheric magnetic features, the longitude ϕ of magnetic elements is time dependent, only λ and t are independent variables. Therefore, the entire surface distribution of the photospheric magnetic field is time dependent even for stable large-scale magnetic features. In other words, the entire surface field distribution is meaningful only with respect to a specific reference time.

Each magnetogram is observed at a CMP time, t_i, and it is the projection of the Earth-side solar surface field on the solar disk. The remapped magnetogram at t_i is the reconstruction of the photospheric field on the Earth-side heliospheric surface, and can be expressed by $B(\lambda, \phi(t_i), t_i)$. At another time t_j, all magnetic elements located along a central meridian at the CMP time t_i (or at the corresponding Carrington longitude, ϕ_c) will be differentially shifted, depending on $(t_j - t_i)$, from this central meridian, and only two elements maintain at their original meridian.

Because both Carrington longitude and the heliographic longitude are time dependent, to avoid any confusion, we define here, for example (as shown in Figure 1), the targe time of 1998.05.23_16:03:30 as the reference time, and denote the corresponding Carrington longitude of 202° at Carrington rotation number of 1936 as "1936_202". The heliographic longitude for the corresponding central meridian is denoted as "1998.05.23:202". For the entire solar surface at this reference time, the heliographic longitude ranges from 1998.05.23:022 to 1998.05.23:022 cover 360° of heliographic longitude. (see the abscissa in three panels of Figure 1).

2.2. Estimation of the effect of the differential rotation on the location of magnetic elements

The differential rotation of solar features, such as spots, plages, and magnetic network, have been studied extensively, and various methods and data selection have led to different rotation rates. These differences have long been interpreted in terms of anchoring depth of these features (Meunier, 2006).

The sidereal or synodic rotation rate of photospheric magnetic features is latitude-dependent and usually expressed as

$$\omega(\lambda) = A + B\sin^2(\lambda) + C\sin^4(\lambda) \tag{1}$$

where λ denotes the heliographic latitude of magnetic elements. The coefficients A, B and C vary depending on the selected magnetic feature and analytic method (e.g., Liu and Zhao, 2009 and references therein). We tried a few sets of the coefficients, and found that the widely-used Snodgrass (1983) rotation rate is equal to the Carrington rotation rate, as expected, at the heliographic latitude of $\pm 16.46^\circ$, and the coronal holes predicted from the synchronic frame obtained using this differential rotation rate agree with observation better than other rotation rates. For the synodic Snodgrass rotation rate, $A = 13.3445$, $B = -1.56154$, and and $C = -2.23407$ in deg/day.

To estimate the effect of the differential rotation, it is necessary to make conversion between the CMP time and the Carrington longitude. In the WSO software system of the Stanford Solar Physics Group, there is a code, "ctimes", that can be used to accurately carry out the convertion between the CMP time and the Carrington longitude. The code is developed about 20 years ago on the basis of ephemeris algorithm and takes consideration the eccentricity of the Earth's orbit. The code introduced a parameter called "Carrington time", the same as Ulrich and Boyden (2006) did but with different way to denote it. In the WSO code, the Carrington time corresponding to, for example, Carrington longitude of 1936:201.74 is denoted as "CT1936:201.74". By

inputing, say, 1998.05.23_16:03:30 to the code, the output of the code s the Carrington time of CT1936:201.74; and by inputing the Carrington time of CT1936:201.74 to the code, we get 1998:05:23_16h:03m:15s, the error from the true CMP time is about 15 second.

To avoid the smearing effect occurred in merging and averaging over multiple observed strips of remapped magnetograms, the heliographic longitudes, that are used to represent meridian lines in remapped magnetograms (see the panel of Figure 1), must be converted to Carrington longitudes. For example, the magnetic elements at latitudes of 16.5° and 40.0° along the heliographic longitude of 1998.05.23:222 are supposed to come, by differential rotating, from the central meridian at the time of 1998.05.23_16:03:30. By using the difference of the two heliographic longitude and Equation (1), we can find out the time interval the two elements take being 1.51469 days and 1.62365 days, respectively. The time when the two elements arrive at the new location will be 1998.05.25_04:24:39 and 1998.05.25_07:22:33. By using the code ctimes, we have Carrinton times of CT1936:181.70 and CT1936:180.06, and Carrington longitudes of 1936:181.70 and 1936:180.06 (1936:182 and 1936:180). All remapped magnetograms over one solar rotation can be corrected using the top panel of Figure 2, where the blue curves show the source Carrington longitude of magnetic elements needed to make the "synoptic chart without the smearing effect" (the same as the "Differential Rotation Corrected" or "DRC" charts in UB06), as shown in the second panel of Figure 2.

As mentioned in Section 1, the synoptic chart is diachronic in nature. To construct an entire surface distribution of photospheric magnetic field at a target time, it is necessary to find out CMP times corresponding to Carrington longitudes and the time difference of the CMP times from the target time. After obtaining the time difference for every Carrington longitude in a synoptic chart, the shift in heliographic longitude each magnetic element subjected can be estimated based on the latitude

the element located and Equation (1). The third panel in Figure 2 shows the effect of the differential rotation on the location of magnetic elements. The red vertical line in the center of the third panel denotes the Carrington longitude of 1936:202° which corresponds to the target time of 1998.05.23_16:03:30 and the reference heliographic longitude of 1998.05.23:202° at the reference time of 1998.05.23_16:03:30. The blue vertical lines denote the Carrington longitudes corresponding to other CMP times. The difference of the blue vertical lines from the central red vertical line is the CMP time difference. Each black or red curve is the locus of heliographic longitudes calculated using the time difference of each inverted CMP time from the reference time. The two horizontal lines denote locus of latitudes where the differential rotation rate equals the Carrington rotation rate. The longitudinal difference of a curve from the vertical blue line that intersects the curve denotes the shift of the magnetic elements. As shown in the panel, all blue vertical lines that intersect with all black curves are located within the 1936:202° centered synoptic chart, and there are four corners where no black curve occurs, demonstrating that the magnetic elements in the synoptic chart cannot be used to completely fill up the entire solar surface at any instant within the period of the rotation.

As expected, the longitude shift depends on the latitude of magnetic elements and the distance of each blue line from the central red line. For the distance greater than 50°, a shift of 10° occurs at most of latitudes above ±30°, indicating the significant effect of the differential rotation included in the synoptic chart component of the synoptic frmae.

2.3. Construction of magnetic synchronic maps and synchronic frames

To cover entire solar surface, more observational data than one solar rotation are needed. As shown by the red curves, the left (right) quadrant outside the synoptic chart that occurs before Carrington longitude 1935:112 (after 1936:22) are needed for filling

up the right (left) blank corners (see the top panel).

The magnetic field distribution will be changed because of the shifts of heliographic longitudes relative to their original meridian line. To obtain the magnetic field distribution in heliographic coordinates, we displace magnetic elements at each blue vertical line to corresponding red or black curves and then get the neuboring averages of the moved magnetic elements at the same latitude around each heliographic longitude.

The bottom panel of Figure 2 shows the MDI magnetic synchronic map, the same as the "Snapshot heliographic map" in UB06. It centers at the heliographic longitude of 1998.05.23:202.°, as shown by the vertical red line and obtained using data of the extended synoptic charts (the second panel). It can be considered as the instantaneous magnetic field distribution over the whole solar surface at the time of 1998.05.23_16.03.30 if the evolution of the photospheric magnetic field in the period of time is caused purely by the differential rotation.

The synchronic frame is thus obtained by merging the remapped magnetogram (the top panel of Figure 1) with the synchronic map (the bottom panel of Figure 2).

3. The effect of differential rotation on the distribution of the field strength and polarity structures

To see if the technique developed here works we first compare the field strength distribution between the synchronic map and synoptic chart.

Figure 3 displays the longitudinal variation of magnetic field strength at latitudes of $-84°$, $-60°$, $-30°$, $-16°$, and $0°$. The blue (red) lines in all panels denote the longitudinal variation in the synchronic (synoptic) frames. As expected, there is no shift between the blue and red lines at latitude of $16°$, where the differential rotation rate is the same as the Carrington rotation rate. Above (below) the latitude of $16°$ the blue line significantly shifts, relative to the red line, toward (away from) the central black

vertical line from two sides. The shift increases as the heliographic longitude aways from the cental black vertical line and as the latitude increases.

The effect of the differential rotation on large-scale magnetic polarity distributions should also be detectable. Figure 4 shows a quantitative sketch of the effect. The rectangles bound by thick (thin) line denote the areas occupied by magnetic structures in the synchronic map (synoptic chart). Depending on the latitude and the longitudinal distance from the center, the thick line rectangles, relative to the thin line rectangles, displace toward the center with their upper parts shear more than the lower parts and their rear parts move more than front parts.

Such differences are perceptible in the bottom panel of Figure 2. All active regions away from the red line in the panel show a displacement toward the red line with respect to the top panel. For instance, the active regions located at $\pm 30^\circ$ of latitude and 1998.05.23_350° of longitude moved about 5° leftward relative their counterpart in the bottom panel of Figure 1. In addition, the active region in northern (southern) hemisphere in the bottom panel of Figure 2 shows a slight counter clock-wise (clock-wise) rotation with respect to the bottom panel of Figure 1. The structures in the east side shows an opposite rotation. This tendency of rotation is consistent with Figure 4.

4. Effect of differential rotation on modeled coronal structures

To see the Effect of differential rotation correction on modeled coronal structures, we compute the open field regions and the source surface neutral line by inputing the synchronic and synoptic frames into the potential field-source surface model.

The top two panels of Figure 5 are the synoptic and synchronic frames. Overplotted are the photospheric polarity inversion lines of large-scale field (green curves). Between the two panels, differences like those found in Figures 3 and 4 also appear in the frames outside the rectangle bound by dashed lines. The displacing, tilting and shrinking of the positive (white) and negative (black) regions in the second panel indicate the effect of

the differential rotation on the distribution of magnetic polarity structures.

What is the effect of this difference on the calculated coronal field, specifically, on modeled coronal holes and the base of the heliospheric current sheet (HCS)?

The bottom two panels of Figure 5 display positive and negative (blue and red) open field regions, the source surface field strength distribution (see contours in grey images) and the neutral lines (black curves). The source surface is located at 2.5 solar radii and the principal order of the spherical harmonic series used in the calculation is 45. The green line in the bottom panel is the same as the neutral line in the third panel. The difference between the two neutral lines in the bottom panel is caused by the correction of differential rotation. The difference of calculated coronal holes between the two panels are also evident both in the portion outside the the rectangle and within the rectangle.

Figure 5 shows that although the correction changes the photospheric field distribution only in the synoptic map component, i.e., the portion outside the rectangle, calculated coronal holes and the HCS are changed in the portion within the rectangle as well as in the portion outside the rectangle.

To see whether or not the magnetic synchronic frame represents a better instantaneous whole surface distribution of the photospheric magnetic field than the synoptic frame, it is necessary to compare the modeled coronal and heliospheric structures overlying the rectangle with observations made at the same time.

Since the synchronic frame is supposed to be a better proxy for the global distribution of the photospheric field at the target time, the coronal structure and the HCS to be compared must be observed near the same time.

The outlines in Figure 6 show the boundary of 1083 nm coronal holes observed at 1998.05.23_17:13 by the NSO Vacuum Telescope of the Kitt Peak Observatory. It is shown that both the blue and red foot point areas calculated using synchronic frame cover larger polar hole area than that using the synoptic frame, though the improvement

is not dramatic. That the improvement is not dramatic may be understood because the modeled coronal hole is governed mainly by its underlying magnetic field and what is corrected is the magnetic field not underlying the coronal hole.

5. Summary and Discussion

We have shown that the magnetic elements from a magnetic synoptic chart cannot be used to fill up the whole solar surface at any time within one Carrington rotation period because of the differential rotation of magnetic features.

By correcting the effect of differential rotation included in the Carrington synoptic chart of the photospheric magnetic field, we first obtain the synoptic chart without smearing, the same as the "DRC synoptic chart" of UB06 and then improve the synoptic chart from diachronic to synchronic to obtain the "synchronic map", or the "snapshot heliographic map" in UB06, which covers whole solar surface and represents a better proxy of the whole surface distribution of the photospheric magnetic field at a target time.

It is found that the effect of avoiding smearing on the polarity pattern and field distribution is not significant. This result may be understood. As shown in the top panel of Figure 2, the smearing effect is heavily depends on the angular width of the strips. For strips with central meridian angles larger than about $\pm 20^\circ$ the smearing effect on the synoptic chart with grid spacing of $360x180$ becomes significant (Ulrich and Boyden, 2006), and when the central meridian angles smaller than about $\pm 10^\circ$, the shift of apparent Carrington longitudes from heliographic longitudes is detectable only for magnetic elements located above latitude of $\pm 50^\circ$ and the shift is only about a couple of degrees . It implies that for most of magnetic elements within the strips of $\pm 10^\circ$ with spatial resolution of 1° , their shift is not detectable. Since the high-candence MDI and HMI observations of magnetograms, the strips with thiner width are used to construct synoptic charts. However, the smearing effect is expected to be significant if

the HMI synoptic maps with grid spacing of $3600x1440$.

By replacing the central part of the synchronic map with the remapped magnetogram at the same time, we obtain the improved synoptic frame, the "synchronic frame".

The comparison of modeled coronal holes and the heliospheric current sheet obtained using the synoptic frame with that using the synchronic frame shows detectable changes in the modeled coronal structures. It is further shown that the modeled coronal holes using the synchronic frame agree with observation of coronal holes better than using the synoptic frame. The results show that the effect of differential rotation on the surface distribution of photospheric magnetic field should be corrected in constructing the instantaneous entire surface distribution of magnetic fields. The simultaneously observed different coronal and heliospheric structures located, respectively, underlying spacecraft SOHO, SDO, and the STEREO A and B will be used to further test the synchronic frame.

The evolution of the photospheric magnetic field depends on other ingredients as well as the differential rotation. Flux transport models that incorporates flux emergence, random-walk dispersal, meridional advection, differential rotation, and removal of flux via cancellation (Schrijver and Derosa, 2003, and references therein), can be used to simulate the evolution of the photospheric magnetic flux from instant to instant over the whole solar surface. The Flux transport models need an initial, instantaneous whole surface distribution of the photospheric magnetic flux as an input. The magnetic synchronic frame is a better input to the models than the magnetic synoptic chart. What predicted from the models and the magnetic synchronic frame is expected to be closer to the realistic whole-surface distribution than what from the magnetic synoptic chart.

It is generally proceeded to use a specific differential rotation rate obtained from a kind of date selections and an analytic method for producing the synchronic maps. Since

different solar features have different differential rotation rates that are associated with their different anchoring depth. Each kind of coronal structures may be associated with their own specific photospheric magnetic features. Therefore, to better model a specific coronal structure, the synchronic frame, as the input to data-based models, should be obtained by improving the synoptic chart and the synoptic frame using the differential rotation rate that is specifically associated with this kind of coronal structure. In addition, the differential rotation rate of solar features may be solar cycle dependent, as found by Meunier (2005). It is worth to study the possibility for further improving the sychronic map and the synchronic frame.

6. Acknowledgments

References

Bumba, B. and R. Howard, *Astrophys. J., 141*, 1502, 1965.

Hoeksema, J. T., J. M. Wilcox, and P. H.Scherrer, *J. Geophys. Res., 88*, 9910, 1983.

Levine, R. H., *Solar Phys., 51*, 345, 1977.

Liu, Y. and J. Zhao, Solar Physics, 260(2), 289, 2009.

Meunier, N., *Astron. & Astrophys., 436*, 1075, 2005.

Pevtsov, A. A. and S. M. Latushko, *Astrophys. J., 528*, 999, 2000.

Schrijver, C. J. and DeRosa, M. L., *Solar Physics, 212*, 165, 2003.

Ulrich, R. K. and J. Boyden, *Solar Phys., 235*, 17, 2006.

Zhao, X. P., J. T. Hoeksema, P. H. Scherrer, *The Proceedings of the Fifth SOHO Workshop at Oslo*, SH-404, p. 751, 1997.

Zhao, X. P., J. T. Hoeksema, P. H. Scherrer, *J. Geophys. Res., 104*, p. 9735, 1999.

Zhao, X. P., J. T. Hoeksema, P. H. Scherrer, *Astrophys. J., 538*, 932, 2000.

X. P. Zhao, W. W. Hansen Experimental Physics Laboratory, Stanford University, Stanford, CA 94305-4085. (e-mail: xuepu@quake.stanford.edu)

J. T. Hoeksema, W. W. Hansen Experimental Physics Laboratory, Stanford University, Stanford, CA 94305-4085. (e-mail: jthoeksema@solar.stanford.edu)

P. H. Scherrer, W. W. Hansen Experimental Physics Laboratory, Stanford University, Stanford, CA 94305-4085. (e-mail: phscherrer@solar.stanford.edu)

Received _____

Second Version: 2 Oct. 2010

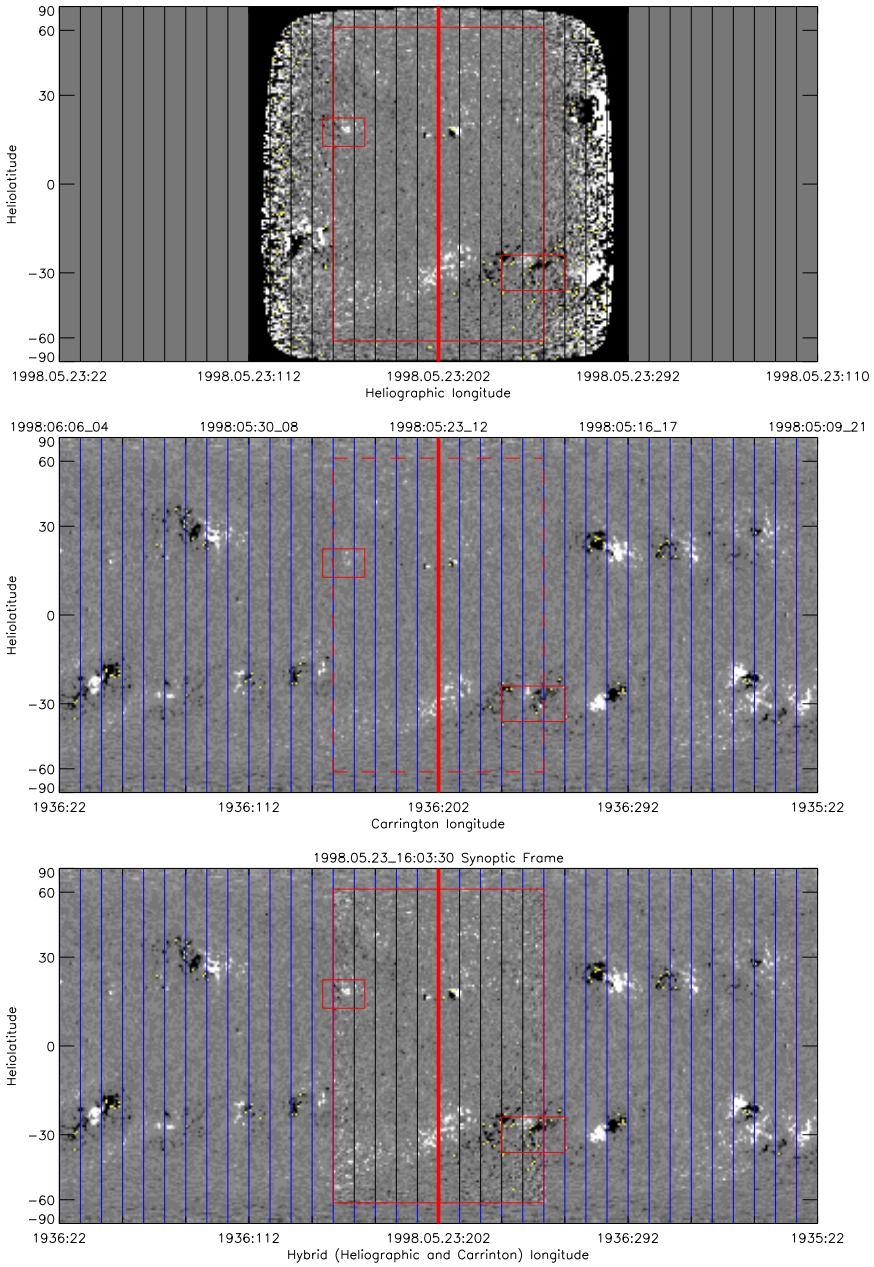

Figure 1. Construction of the synoptic frame of the photospheric magnetic field (bottom panel) using a remapped magnetogram (top panel) and an non-traditional synoptic chart (middle panel). Black and blue vertical lines denote, respectively, Heliographic and Carrington longitudes. The abscissa in bottom panel is in hibrid manner, using heliographic longitude for magnetogram component, and using Carrington longitude for synoptic chart component.

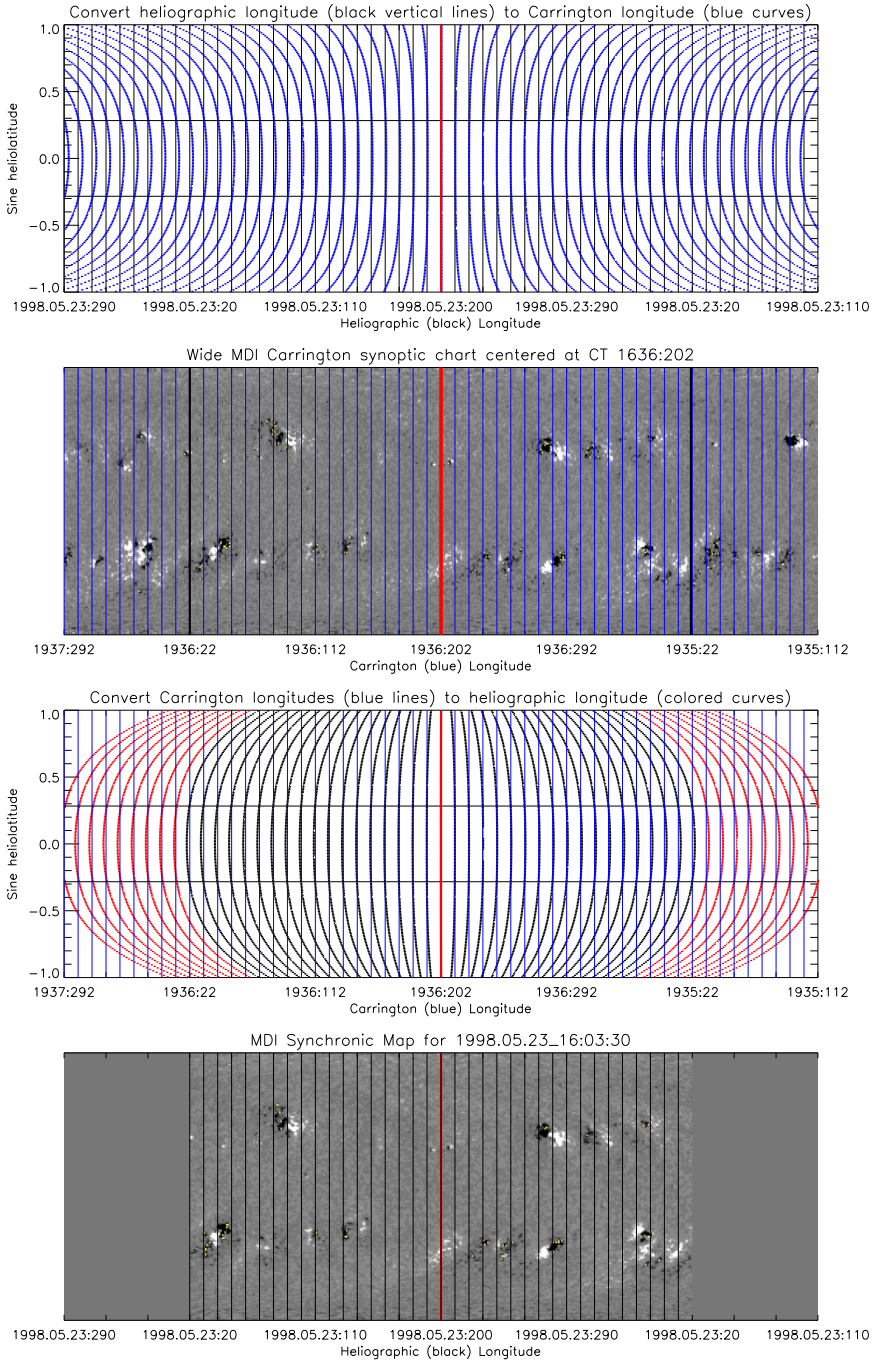

Figure 2. Construction of synchronic charts (bottom panel) from non-traditional synoptic charts (top panel). The abscissa in top (bottom) panel is in Carrington (Heliographic) longitude (see text for details).

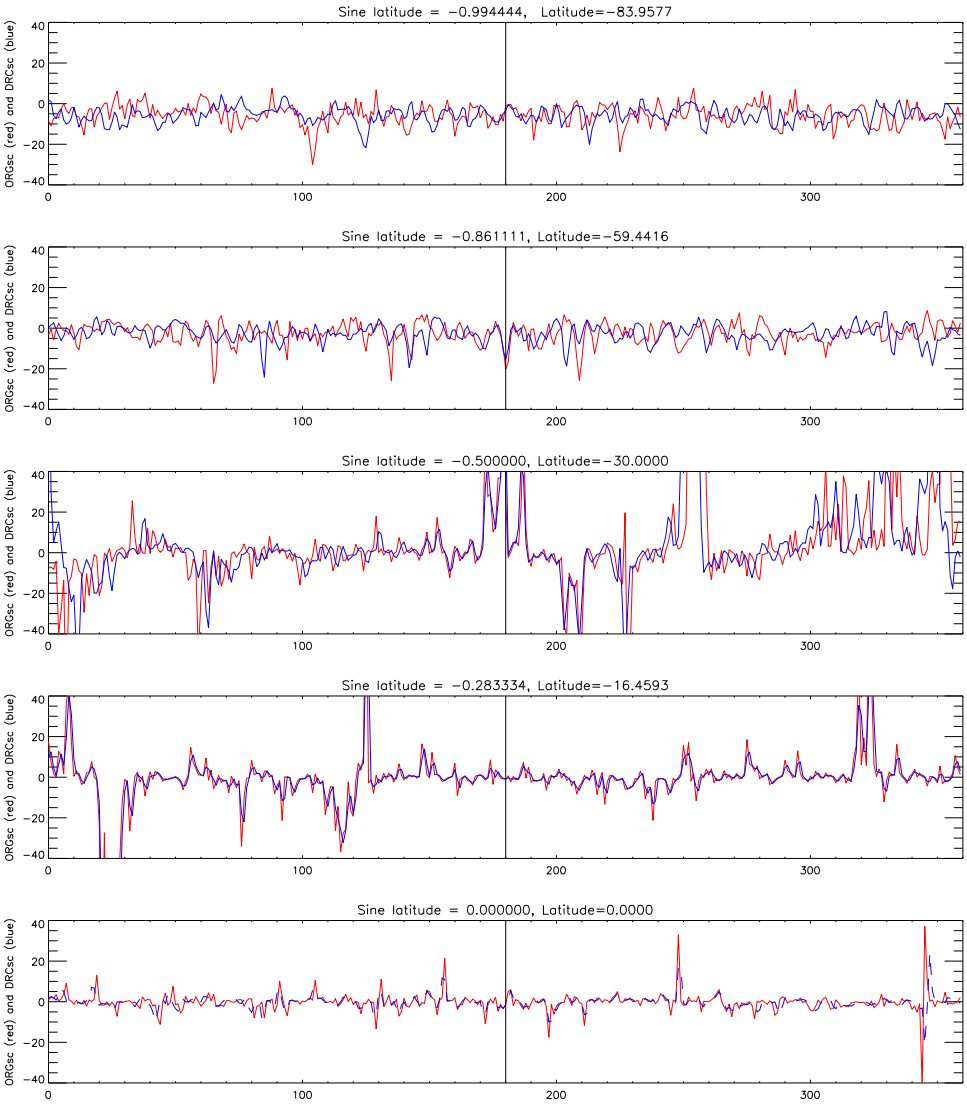

Figure 3. Comparison of the longitudinal variation of magnetic field at latitudes of 0, 16, 30, 60 and 84° (from bottom to top) between the synoptic chart (red lines) and the synchronic map (blue lines).

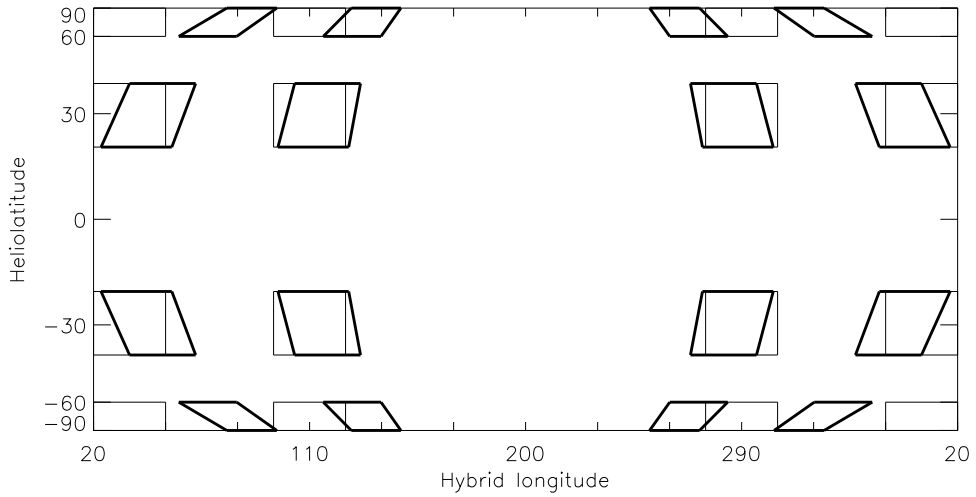

Figure 4. Comparison between non-traditional synoptic charts (thin outlines) and synchronic charts (thick outlines), showing the effect of differential rotation on magnetic structures.

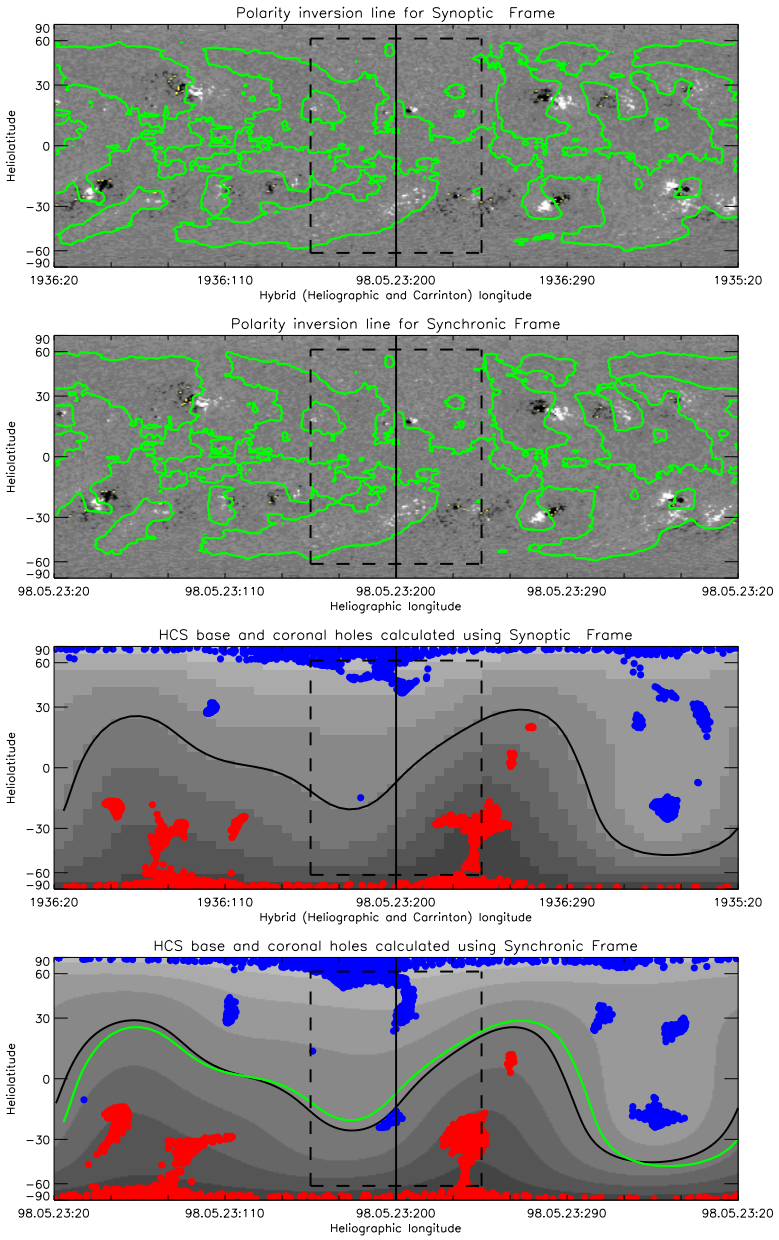

Figure 5. Comparison between synoptic frames (the first panel) and synchronic frame (the second panel). The green lines in the two panels are polarity inversion lines of large-scale photospheric field. The third and fourth panels shows the foot-points of open field lines (blue-positive and red-negative) and source surface neutral lines calculated using the first and second panels, respectively.

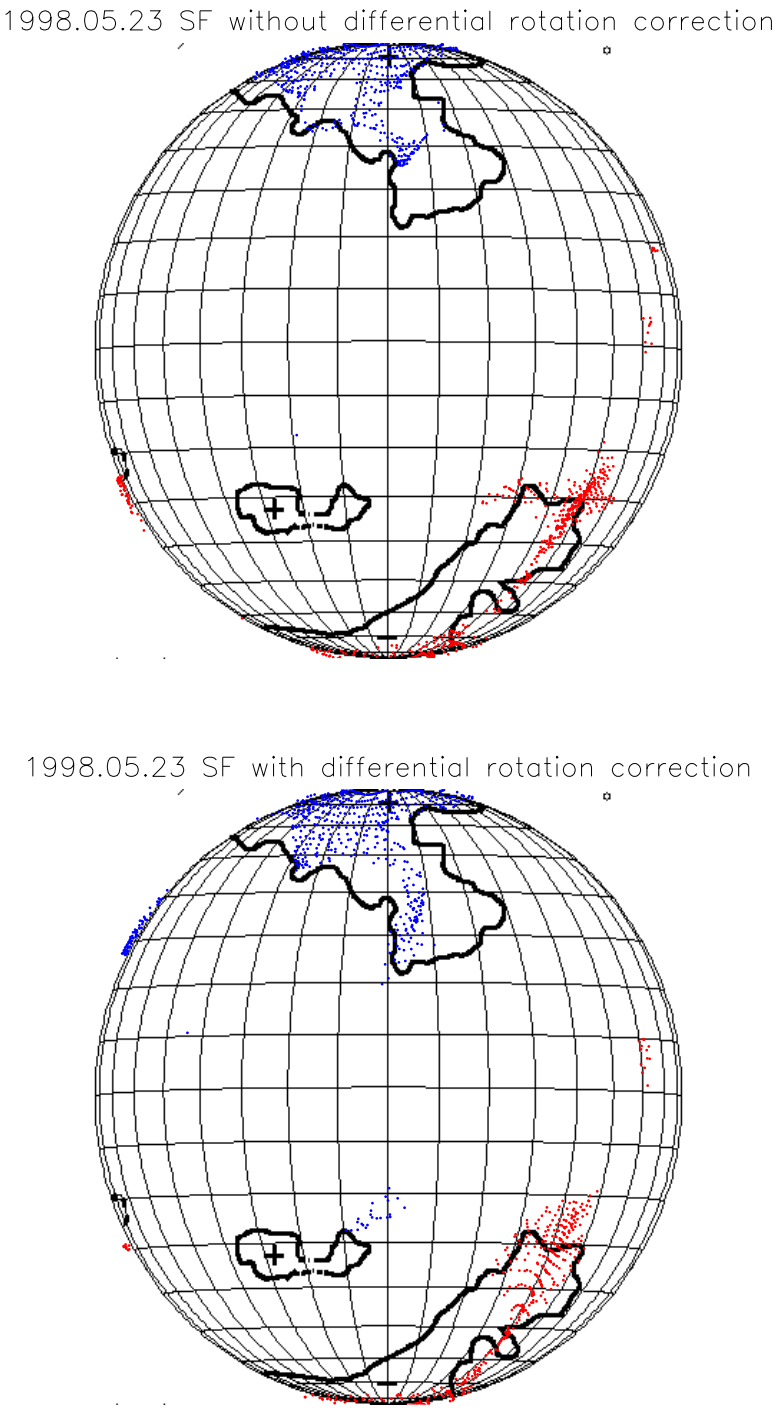

Figure 6. Comparison of open field regions calculated using the 1998.05.23_16:03:30 synoptic frame and the synchronic frame with KPNO He 1083.0 nm coronal holes observed at 1998.05.23_17.43.